AFRL-RZ-WP-TP-2011-2163

FLAME STRUCTURE OF VITIATED FUEL-RICH INVERSE DIFFUSION FLAMES IN A CROSS-FLOW (Postprint)

David Blunck, Amy Lynch, Joseph Zelina, and James R. Gord
Combustion Branch
Turbine Engine Division

Stanislav Kostka and Sukesh Roy
Spectral Energies LLC

Marc Polanka
Air Force Institute of Technology

Scott Stouffer
University of Dayton Research Institute

DECEMBER 2011

AIR FORCE RESEARCH LABORATORY
PROPULSION DIRECTORATE
WRIGHT-PATTERSON AIR FORCE BASE, OH 45433-7251
AIR FORCE MATERIEL COMMAND
UNITED STATES AIR FORCE

REPORT DOCUMENTATION PAGE

Form Approved
OMB No. 0704-0188

1. REPORT DATE *(DD-MM-YY)*	2. REPORT TYPE	3. DATES COVERED *(From - To)*
December 2011	Conference Paper Postprint	10 December 2011 – 10 December 2011

4. TITLE AND SUBTITLE
FLAME STRUCTURE OF VITIATED FUEL-RICH INVERSE DIFFUSION FLAMES IN A CROSS-FLOW (Postprint)

5a. CONTRACT NUMBER
IN-HOUSE

5b. GRANT NUMBER

5c. PROGRAM ELEMENT NUMBER
62203F

6. AUTHOR(S)
David Blunck, Amy Lynch, Joseph Zelina, and James R. Gord (Turbine Engine Division, Combustion Branch (AFRL/RZTC))
Stanislav Kostka and Sukesh Roy (Spectral Energies LLC)
Marc Polanka (Air Force Institute of Technology)
Scott Stouffer (University of Dayton Research Institute)

5d. PROJECT NUMBER
3048

5e. TASK NUMBER
04

5f. WORK UNIT NUMBER
304804CC

7. PERFORMING ORGANIZATION NAME(S) AND ADDRESS(ES)
Turbine Engine Division, Combustion Branch (AFRL/RZTC)
Propulsion Directorate
Air Force Research Laboratory
Wright-Patterson Air Force Base, OH 45433-7251
Air Force Materiel Command, United States Air Force

- Spectral Energies LLC
- Air Force Institute of Technology
- University of Dayton Research Institute

8. PERFORMING ORGANIZATION REPORT NUMBER
AFRL-RZ-WP-TP-2011-2163

9. SPONSORING/MONITORING AGENCY NAME(S) AND ADDRESS(ES)
Air Force Research Laboratory
Propulsion Directorate
Wright-Patterson Air Force Base, OH 45433-7251
Air Force Materiel Command
United States Air Force

10. SPONSORING/MONITORING AGENCY ACRONYM(S)
AFRL/RZTC

11. SPONSORING/MONITORING AGENCY REPORT NUMBER(S)
AFRL-RZ-WP-TP-2011-2163

12. DISTRIBUTION/AVAILABILITY STATEMENT
Approved for public release; distribution unlimited.

13. SUPPLEMENTARY NOTES
PAO case number: 88ABW-2011-0362, cleared 28 January 2011. The U.S. Government is joint author of the work and has the right to use, modify, reproduce, release, perform, display, or disclose the work. Presented at the 2011 7th US National Combustion Meeting organized by the Eastern States Section of the Combustion Institute and hosted by the Georgia Institute of Technology, Atlanta, GA March 20-23, 2011. Document contains color.

14. ABSTRACT
Fuel-rich streaks or dissociated combustion products exiting from gas turbine combustors may react with jets of turbine vane cooling air. These fuel-rich vitiated inverse diffusion flames can potentially cause structural failure of turbine vanes due to the excessive heat fluxes. In this study OH planar laser induced fluorescence measurements are conducted in fuel-rich vitiated flows advecting over a flat plate with a row of cooling holes normal to the surface. Vitiated conditions are generated by burning propane at equivalence ratios between 1.1 and 1.4 in a well-stirred reactor located upstream of the test section. The structures of the flames (i.e., spatially-resolved species measurements) are compared for different equivalence ratios and blowing ratios. It is observed that the flames generated by the cooling air are inherently unsteady, with the standard deviation of the flame tip location varying by as much as 35%. The distance downstream of the slot where the flame tip was observed varies by 20% or less (with respect to the average) for a factor of 20 increase in the blowing ratio. The separation between the flame and the wall is similar for blowing ratios between 1 and 5, but increases for a blowing ratio of 10. Changing the equivalence ratio of the vitiated flow has little effect on the location where flames are observed.

15. SUBJECT TERMS
turbulent flames

16. SECURITY CLASSIFICATION OF:			17. LIMITATION OF ABSTRACT:	18. NUMBER OF PAGES	19a. NAME OF RESPONSIBLE PERSON (Monitor)
a. REPORT	b. ABSTRACT	c. THIS PAGE			David Blunck
Unclassified	Unclassified	Unclassified	SAR	16	19b. TELEPHONE NUMBER *(Include Area Code)* N/A

2011 7th US National Combustion Meeting
Organized by the Eastern States Section of the Combustion Institute
and Hosted by the Georgia Institute of Technology, Atlanta, GA
March 20-23, 2011

Flame Structure of Vitiated Fuel-rich Inverse Diffusion Flames in a Cross-Flow

David Blunck[1], Stanislav Kostka[2], Amy Lynch[1], Marc Polanka[3], Scott Stouffer[4], Sukesh Roy[2], Joseph Zelina[1], James R. Gord[1]

[1]Air Force Research Laboratory, Propulsion Directorate, WPAFB, OH
[2]Spectral Energies LLC., Dayton, OH
[3]Air Force Institute of Technology, WPAFB, OH
[4]University of Dayton Research Institute, Dayton, OH

Fuel-rich streaks or dissociated combustion products exiting from gas turbine combustors may react with jets of turbine vane cooling air. These fuel-rich vitiated inverse diffusion flames can potentially cause structural failure of turbine vanes due to the excessive heat fluxes. In this study OH planar laser induced fluorescence measurements are conducted in fuel-rich vitiated flows advecting over a flat plate with a row of cooling holes normal to the surface. Vitiated conditions are generated by burning propane at equivalence ratios between 1.1 and 1.4 in a well-stirred reactor located upstream of the test section. The structures of the flames (i.e. spatially-resolved species measurements) are compared for different equivalence ratios and blowing ratios. It is observed that the flames generated by the cooling air are inherently unsteady, with the standard deviation of the flame tip location varying by as much as 35%. The distance downstream of the slot where the flame tip was observed varies by 20% or less (with respect to the average) for a factor of 20 increase in the blowing ratio. The separation between the flame and the wall is similar for blowing ratios between 1 and 5, but increases for a blowing ratio of 10. Changing the equivalence ratio of the vitiated flow has little effect on the location where flames are observed.

1. Introduction

Requirements for increased efficiency and thrust-to-weight ratio are resulting in more compact gas turbine combustors [1] which operate at higher temperatures and pressures. With these advances the likelihood of fuel-rich combustion products entering the turbine increases, either from incomplete reactions in the combustor, or dissociation of the exhaust species [2,3]. Unburned hydrocarbons, carbon monoxide, hydrogen, and minor species in the vitiated flow can react with the jets of air used to cool the vanes. These inverse diffusion flames in a vitiated cross-flow increase the heat flux to the turbine vanes and may lead to catastrophic failure of components. Several experimental and computational studies have quantified the heat flux and cooling effectiveness when these flames are present [3-6]. Typically changes in the heat flux and cooling effectiveness have been reported as a function of the Damköhler number (*Da*), equivalence ratio (Φ), cooling hole geometry, blowing ratio, and potential enthalpy release. Inverse diffusion flames in a vitiated cross-flow have been further studied for application to staged-air burners in low NO_x emitting furnaces. To study these flames, Partridge and Laurendeau had products from a fuel-rich ethane-air flame flow through a chimney where two (opposed) jets of air were injected. Changes in NO and NO_x emissions were measured and

correlated to the laminar or turbulent nature of the flames and changes in mixing between the vitiated flow and the air jets [7]. Clausing et al. used a similar experimental arrangement to develop a Peclet number correlation to predict the occurrence of flame lift-off. The correlation provided a reasonable estimate of the air jet velocity at which lift-off was observed [8]. In both the turbine film cooling and staged burner studies the shape and structure of inverse diffusion flames in a vitiated cross-flow have been neglected. This information is needed for developing and validating robust computational models, optimizing techniques for controlling the flames, or minimizing pollutant formation.

Literature relevant to inverse diffusion flames and jets in a cross-flow is now summarized. Wu and Essenhigh measured the temperature and species of methane, propane and acetylene inverse diffusion flames to understand the structure and stability of these flows. Reasonable agreement was noted between the data and predictions using the Burke and Schumann flame sheet concept developed for normal diffusion flames, suggesting mathematical similarity between the two types of flames [9]. Shaddix et al., reported that the relative positions of OH, PAH, and soot were similar between steady inverse and normal diffusion flames. OH fluorescence signals were comparable between the two types of flames [10].

Despite the similar structure, inverse diffusion flames tend to be less stable than normal flames. Blow-off of inverse diffusion methane flames was reported at air supply velocities near 1 m/s or less (Reynolds numbers < 1000) for an 11 mm diameter (inner) jet. Lifted flames prior to blow-off were not reported [9]. Broadway et al. reported blowout velocities near 100 m/s for a normal methane diffusion flames with a similar diameter (8 mm) [11]. Clausing et al., attributed the typically lower blow-off velocity for inverse diffusion flames to the smaller amount of surrounding gas which needs to be entrained for stoichimetric conditions to be present [8].

The stability and entrainment of transverse jets in a cross-flow has been the focus of considerable research in the combustion and fluid mechanic communities [12-15]. Grout et al. (2011) calculated the stability of transverse jets of hydrogen in a cross-flowing stream of heated air (750 K). The flame stabilized 1.5 to 2 nozzle widths downstream and 3 to 5 nozzle heights above the fuel jet, based on heat release contours. This region corresponds to the lower region of the jet. Locations of peak heat release correspond to regions where the average flow velocity is low and the mixture fraction approaches stoichiometric conditions [14]. McMillin et al., reported time-resolved and average temperature images of a fuel jet exiting into a cross-flowing hot nonoxidizer supersonic flow. Time-resolved images showed pockets of undiluted free stream fluid within the plume. The distinct jet boundaries in the images indicated sharp scalar gradients. The temperature within the lower downstream portion of the plume was nearly uniform indicating efficient mixing, making the region favorable for autoignition [16]. Transverse jets typically have enhanced entrainment relative to a regular jet at a sufficient distance from the nozzle. Muppidi and Mahesh [12,17] performed direct numerical simulations of nonreacting jets in a cross-flow. Prior to a distance of 2 diameters entrainment of the regular jet was found to be equivalent or larger than the transverse jet. At a distance of 6 and 9 nozzle diameters, entrainment of the transverse jet (velocity ratio of 5.7) was approximately 2 and 3 times greater (respectively) than a regular jet. Upwards of 90% of the fluid entrained in this region is from the downstream portion of the jet. The changes in entrainment resulted from the pressure gradients which form around the transverse jet. The high pressure region upstream of the jet caused the cross-stream flow to accelerate and the jet deflection. The pressure gradient on

the downstream side of the jet opposed the acceleration of the cross-stream flow and caused the cross-stream to flow toward the jet, thus augmenting the entrainment [12].

The structure and location of flames can be nonintrusively measured using planar laser induced fluorescence of hydroxyl (OH). Measurements of the OH layer within flames has been used by numerous researchers in the past to describe flame front locations [18]. Planar laser induced fluorescence (PLIF) allows two-dimensional information to be determined in a single plane, unlike other techniques such as chemiluminescence imaging which provide line-of-sight measurements. PLIF measurements provide high temporal resolution (order of ns), thus minimizing blurring of flame features. Temperature fields can be obtained through implementing two color OH PLIF with the excitation of multiple OH transitions using two laser sources. Thermometry measurements using OH were originally performed by Cattolica. These measurements were performed by exciting two different OH transitions, giving a representation of the Boltzmann distribution of OH [19]. This Boltzmann distribution dependence on temperature can be determined by using LIFBASE simulations [20]. Many researchers have implemented two-color PLIF for temperature measurements using various OH transition pairs both for averaging and instantaneous measurements [21,22].

Given this literature review and the need to understand the structure and stability of inverse diffusion flames in a vitiated cross-flow, the objectives of this work are as follows:

1) Obtain visible images of inverse diffusion flames in a vitiated cross-flow;
2) Measure OH fluorescence of the flames;
3) Quantify changes in the flame front as the blowing ratio and equivalence ratio are varied.

2. Experimental Arrangement

The experimental arrangement for generating the flames has been reported previously and is now briefly summarized [4,23] Premixed fuel (propane) and air are injected into an atmospheric pressure well-stirred reactor [24] and burned. The combustion products exit the well-stirred reactor and flow through a transition duct, as shown in Fig. 1, prior to entering the film cooling

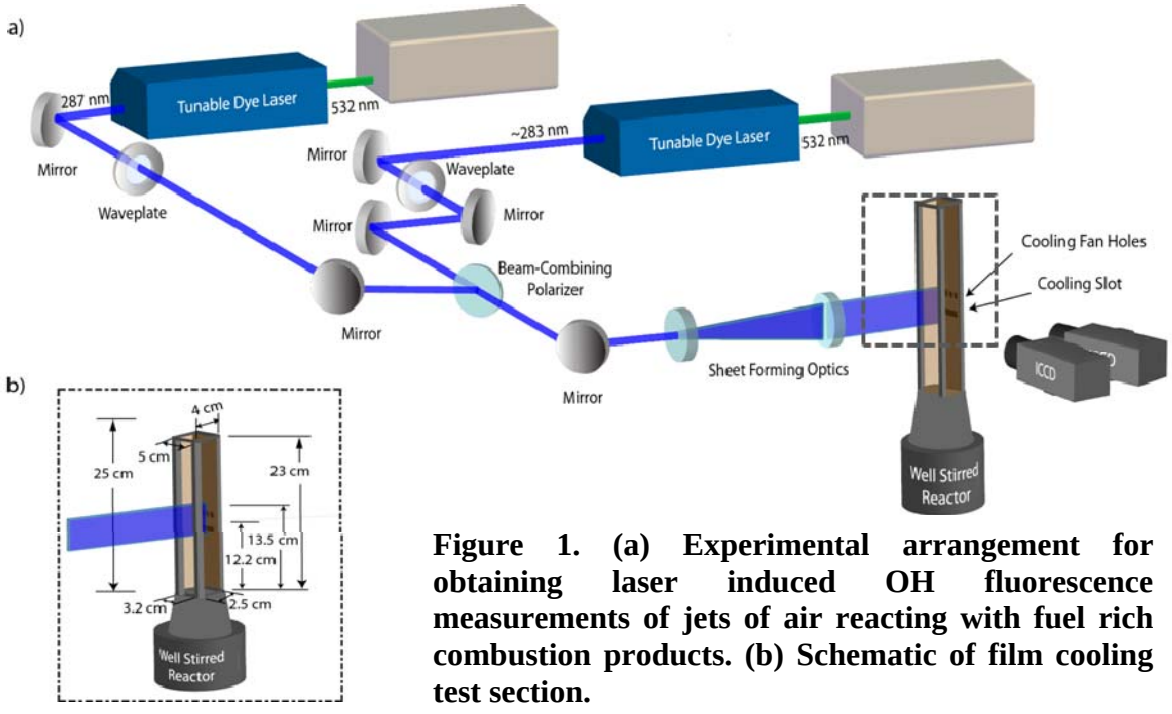

Figure 1. (a) Experimental arrangement for obtaining laser induced OH fluorescence measurements of jets of air reacting with fuel rich combustion products. (b) Schematic of film cooling test section.

article. The transition duct interfaces the circular exit of the well-stirred reactor with the rectangular entrance of the film cooling section. A series of flow straighteners located within the duct reduce the swirl in the vitiated flow as it exits the well-stirred reactor. The transition duct and reactor are lined with ceramics to reduce heat losses from the flow and ensure that the metal housing survives the high temperatures.

The rectangular shaped film cooling section consists of an instrumented metal block on one side with quartz windows on the three other sides, as illustrated in Fig 1(b). The metal block is water cooled (60 g/s) to ensure that the material does not warp. A plenum with a slot machined at one face was inserted into the metal section. The angled slot (30° respect to surface) was 1.3 mm wide and 38 mm long [23]. Slot flows can be approximated as two-dimensional and have been used in the film cooling literature to provide an ideal performance for comparing other hole geometries [25]. The temperature of the air inside the plenum was measured approximately 5 mm from the exit using a type-K thermocouple. Typical values were between 400 and 600 K due to heating by the hot walls of the metal block and external heaters.

The air flow rate through the well stirred reactor and film cooling test article was fixed at 425 SLPM. Propane flow rates were adjusted to obtain the desired equivalence ratios (1.1, 1.2, 1.3, and 1.4). Flow rates were controlled using thermal mass flow meters. The Reynolds number of the vitiated flow at the inlet to the test section was approximately 4000 based on the measured gas temperature, the hydraulic diameter (4.3 cm), and assuming properties of air. The temperature of the vitiated flow was between 1500 and 1600 K at the inlet to the test section. The vitiated products flowed over a step on the metal block approximately 12 cm upstream of the slot to create a turbulent boundary layer. Air flow rates through the cooling holes are reported based on the blowing ratios [25],

$$M = \frac{\rho_j U_j}{\rho_{cf} U_{cf}}, \quad (1)$$

where ρ and U are the density and velocity respectively and the subscripts j and cf represent jet and cross-flow. The blowing ratio was determined from the mass flow rate and the exit area to avoid the added complexity of measuring velocities.

Chemical equilibrium calculations [26] were performed to estimate the species concentrations in the vitiated cross-flow. The calculations were performed at atmospheric pressure and at a temperature of 1650 K, representative of the conditions at the inlet to the film cooling section. The results are reported in Table 1. Increasing the equivalence ratio increases the carbon monoxide and molecular hydrogen in the flow and decreases the carbon dioxide as expected. It is expected that radicals important for ignition and oxidation (e.g. H and OH) are present in the flow.

Table 1. Calculated mole fractions of products in the cross-flow.

	Mole Fraction						
Equivilence Ratio	**CO**	**CO_2**	**H_2**	**H_2O**	**OH ($x10^3$)**	**H ($x10^3$)**	**N_2**
1.1	0.03	0.1	0.01	0.15	0.01	0.01	0.70
1.2	0.05	0.08	0.03	0.15	-	0.01	0.68
1.3	0.07	0.07	0.04	0.15	-	0.02	0.67
1.4	0.08	0.06	0.06	0.14	-	0.02	0.065

3. Laser Diagnostics

The experimental arrangement includes two tunable laser sources, tuned to different OH transitions, as shown in Fig. 1. The lines chosen are the $Q_1(14)$ and $Q_1(5)$ of the $A^2\Sigma^+ \leftarrow X^2\Pi$ (1,0) band of OH. Kostka [27] found that these lines can be used to produce temperature accuracies of about 4.5% when absorption and spectral overlap corrections are implemented. The two color PLIF technique provides temperature measurements in the presence of OH, particularly in the reaction region of the inverse diffusion flames. Temperature measurements become more difficult for conditions where little to no OH is present in the flow due to the weak $Q_1(14)$ transition; however, OH concentration measurements for the strong $Q_1(5)$ transition still provide flame structure information for low concentrations. In the present work, measurements of the $Q_1(5)$ transition alone are reported and used to characterize the location of the flame. The $Q_1(14)$ transition will be incorporated in future work, as discussed in the remainder of the current section and in the future work section. Due to the insensitivity of the $Q_1(5)$ transition to temperature between 1400 and 2400 K Boltzmann fraction corrections for temperature were avoided.

A Spectra Physics Pro 290 and Quanta Ray 250 Nd:YAG laser were used to pump a Sirah Cobra Stretch and Continuum ND6000 Dye laser, respectively. Laser repetition rates were each 10 Hz. The approximately 565.5 nm output of the Sirah dye laser was passed though a Sirah autotracker frequency conversion unit producing a doubled output of 282.75 nm at an energy of about 9 mJ per pulse for the $Q_1(5)$ transition. The 572.9 nm output from the Continuum dye laser was passed through a BBO crystal within an Inrad Autotracker III unit and then through a Pellin Broca prism to spatially separate the 286.4 nm beam used to excite the $Q_1(14)$ transition of OH. Wavelength measurements were performed using a High Finesse WS-7R wavemeter, and transition overlap was further maximized by measuring the OH fluorescence in a calibration Hencken burner [27].

Before passing to the experimental apparatus the two laser beams were spatially overlapped using a combination of half wave plates, turning mirrors and a thin film polarizer. A half wave plate was used to rotate the polarization of the laser beam generated by the Sirah to reflect off the surface of the polarizer. The second, continuum, beam was also passed through a half wave plate to ensure horizontal polarization. This horizontally polarized beam was transmitted through the thin film polarizer to ensure spatial overlap. Both beams were passed through a series of turning mirrors and sheet forming optics connected to a motorized translational stage. After passing through the optics the laser sheets were about 5 cm in height at the test section. The stage provided the ability to scan the beam across the experimental test section, while also allowing for measurements in the Hencken burner flame placed alongside the experimental apparatus.

Fluorescence collection was performed using two Princeton Instruments PI-MAX 2 ICCD cameras. Timing of the cameras was synchronized to the laser pulses using a Labsmith programmable timing generator and the camera programmable timing controllers. Pulse separation was set to 2 μs to ensure rotational and vibrational relaxation of the OH between pulses. The intensifier gate width on each camera was set to 100 ns to minimize the collection of flame emission. Collection of the fluorescence was performed using a 105 mm UV objective lens together with a band-pass filter to help eliminate any collection of laser scatter. Semrock Brightline filters centered at 320nm with a bandwidth of 40nm were used, providing 80% transmission of the OH fluorescence. The cameras were placed on a motorized translational

stage, set parallel to the launching optics so that scanning is possible. Measurements in this paper involved measurements along the centerline of the experimental apparatus.

4. Discussion and Results

Figure 2 shows visible images of the flames anchored to the air jets exiting from the slot with blowing ratios of 0.5, 2, and 4. The equivalence ratio of the vitiated flow is 1.3. Chemical equilibrium calculations of the species in the flow based on the equivalence ratio and measured temperature at the inlet to the film cooling section are reported in Table 1. The images were acquired using a Sony Alpha 100 DSLR camera fitted with a macro lens. The blue visible radiation in the figure is chemiluminescence from CH* radicals. The surrounding lighter (orange) color is radiation emitted from soot in the flow, ceramic particles which ablate off the liner, and the hot rig surfaces. The flames are lifted away from the wall and downstream of the slot. The flame length increases as the blowing ratio increases as a result of the greater mass of air which reacts.

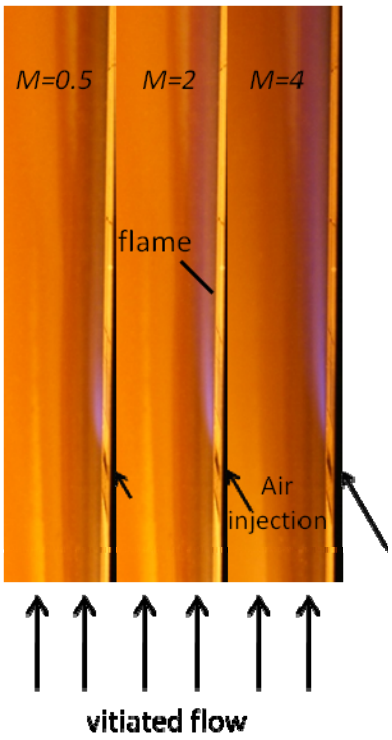

Figure 2. Visible radiation emitted from fuel rich vitiated cross-flow reacting with cooling air exiting from a slot with blowing ratios (from left to right) of 0.5, 2, and 4.

Ignition of the flames is caused by the second stage of autoignition which results from the chain-branching step,

$$H + O_2 \rightarrow O + OH. \quad \text{(R.1)}$$

At temperatures above approximately 1200 K reaction 1 dominates ignition of hydrocarbons [28]. The high temperature and the hydrogen atoms in the vitiated cross-flow (see Table 1) facilitate reaction 1 and the ignition of the inverse diffusion flames. Ignition occurs on the fuel-rich side of the flammability limits due to the cross-flow being the fuel and at a high temperature. After ignition the carbon monoxide in the cross-flow is oxidized following the reactions reported in the literature [29,30].

The location where the flames stabilize is similar for the different blowing ratios (see Fig. 2). This results from the similar ignition delay times for the flames. Katta et al., reported that a lifted laminar ethylene diffusion flame anchored to the autoignition products formed in the recirculation zone above the burner [31]. It is plausible that the flames reported in this work have a similar stabilization mechanism; the vitiated products in the cross-flow autoignite and anchor the oxidation of the carbon monoxide. The ignition location and where the flame anchors depends primarily on the cross-flow velocity and the ignition delay time (τ) (Ben-Yakar and Hanson, 1998),

$$l = {}^{U_{cf}}/_{\tau}. \quad (2)$$

Changes in the blowing ratio alter the penetration of the jet, but do not affect the ignition delay time, which depends on temperature, pressure, and chemistry, and have little influence on the

cross-flow velocity. Consequently, the location where ignition occurs and the flame stabilizes is similar for the different blowing ratios. This was supported by observations of the flame as the blowing ratio was increased from 4 to 15. Visible radiation from the flame was evident for all conditions and blow-off was not observed, indicating little dependence of flame anchoring on the blowing ratio.

Figure 3 presents instantaneous and average OH fluorescence measurements for flames with conditions equivalent to those in Fig. 2 (M = 0.5, 2, 4) as well as a blowing ratio of 10. All intensities were normalized by a common value (the maximum from all data) for display and comparison purposes. The flames are lifted away from the wall and downstream of the slot. The location where the OH radicals become evident is similar in the average images, comparable to the results in Fig. 2. The location downstream where the flame tip was detected was quantified for 250 instantaneous images at each blowing ratio. The flame front was observed 0.55 cm downstream of the slot, based on the average of all the measurements. The factor of 20 change in the blowing ratio altered the attachment location by 20% or less with respect to the average location. Flames with blowing ratios of 4 and 10 were anchored the farthest (0.65 cm) and closest (0.44 cm) to the slot respectively. The latter observation is attributed to the greater penetration of the jet into the cross-stream. It is noted that the flame lengths are similar for the different blowing ratios in Fig. 3. This is an artifact of the finite height of the laser sheet.

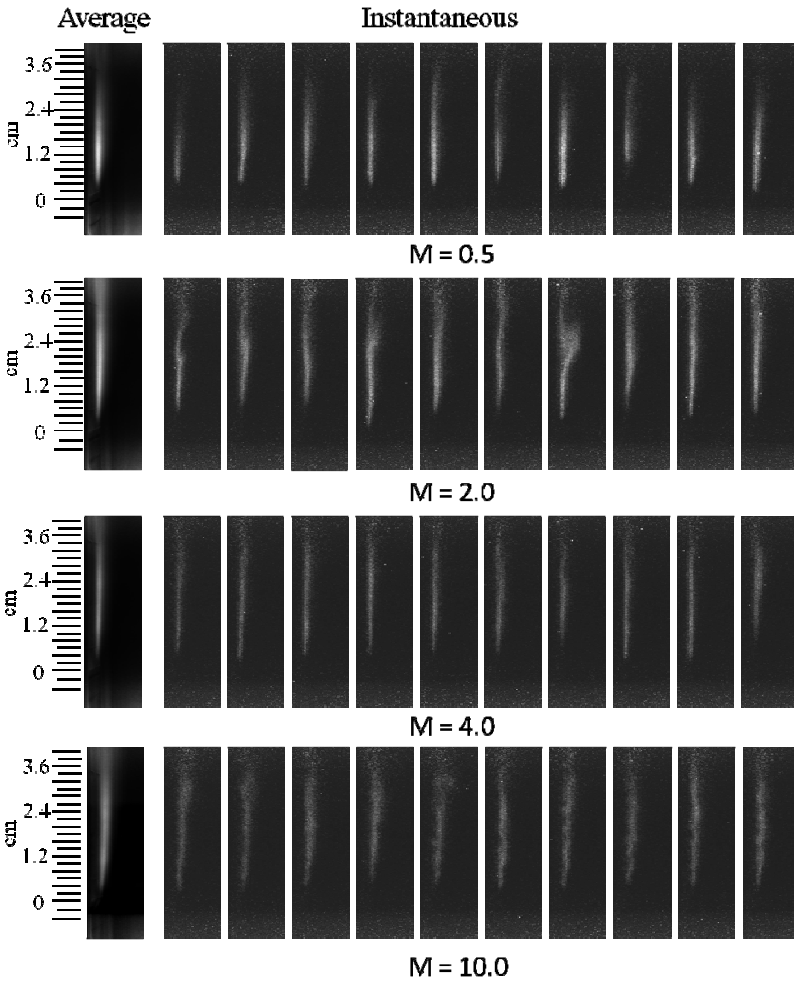

Figure 3. Instantaneous and average OH concentration measurements of flames with blowing ratios of 0.5, 2, 4, and 10 anchored to a slot.

Instantaneous images indicate that the flames are unsteady. The width of the flame front and the downstream location where the reactions anchor fluctuates. The flame anchors between 0.4 and 0.8 cm downstream of the slot in the images. These fluctuations result from the turbulent nature of the cross-flow. The standard deviation of the flame tip location is 25% to 35% of the mean tip location for each blowing ratio. Flames which anchor farther downstream tend to have larger fluctuations in the flame tip. Huang and Yang reported that the stability of burner attached

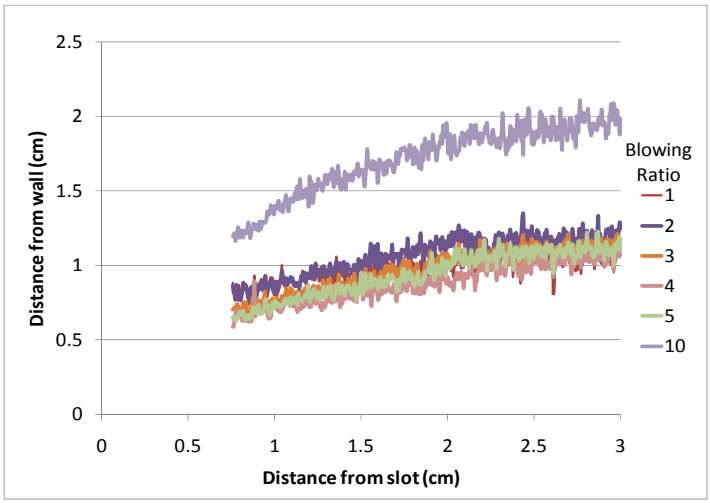

Figure 4. Distance between wall and location of peak OH concentration at axial locations between 0.75 and 3 cm downstream of the slot.

distance downstream due to the jet momentum. Between 1 and 3 cm downstream of the slot the distance from the wall increases by approximately 25% to 50% for the various blowing ratios. The location of the flames with blowing ratios between 1 and 4 is similar. Increasing the blowing ratio to 10 causes the separation distance of the flame to increase by 60-100% relative to the other flames. The greater momentum causes the air jet to penetrate farther into the cross-flow.

Average OH concentrations acquired of the slot flames (M = 4) for equivalence ratios of 1.1 – 1.4, and are reported in Figure 5. The intensity is normalized by a common value, similar to the other images. The flame fronts for the flames are qualitatively similar. The peak concentrations (brightest color) changes with the equivalence ratio of the vitiated flow. This results from changes in the carbon monoxide concentrations in the flow (see Table 1) and increased absorption of the fluorescence signal by soot in the flow as the equivalence ratio is increased.

jet flames in a cross-flow is influenced by the structures which develop in the flow as a function of the burner obstruction and cross-flow and jet velocities [33].

The mean distance between the wall and the location of peak OH concentration are reported in Fig. 4 for select blowing ratios between 1 and 10. This provides an indication of the changes in the location of the reaction zone for different blowing ratios. Results are reported between 0.75 and 3 cm downstream of the slot, in the region where the signal to noise ratio was the largest. The separation distance between the wall and the flames increases with

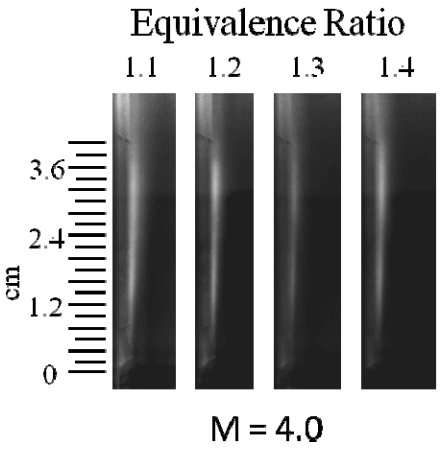

Figure 5. Average OH measurements of flames in vitiated flows with equivilence ratios of 1.1, 1.2, 1.3, and 1.4 with a blowing ratio of 4 anchored to a slot.

5. Summary and Conclusions

OH fluorescence measurements were acquired of inverse diffusion flames in fuel-rich vitiated flows. The blowing ratio was varied between 0.5 and 10. Instantaneous measurements show that the flames are unsteady. Flames which anchor further downstream tend to have larger fluctuations in the flame tip location. Changing the blowing ratio has a minor effect on the location downstream of the slot where the flame tip was observed due to the independence of

ignition location on the velocity of the air jet. Increasing the blowing ratio from 5 to 10 causes the flame to separate farther from the wall due to the increased momentum. Changing the equivalence ratio of the vitiated flow has little effect on the location where flames are observed.

6. Future Work

Future work includes incorporating the two-color PLIF technique described in the laser diagnostics section to obtain temperature measurements and quantify OH concentrations. Measurements will be acquired with varying cross-flow velocities, equivalence ratios, and blowing ratios to assess changes in the ignition location, flame stability, and anchoring position. Two-dimensional modeling of the inverse diffusion slot flames with detailed chemical kinetics will provide insights into the ignition and flame stabilization mechanisms. Nonreacting three-dimensional computational fluid dynamic calculations will be used to understand differences in the entrainment and mixing as the blowing ratio and cooling hole geometry are changed. The numerical modeling will be validated using the measured temperature and OH concentration.

7. Acknowledgments

Mike Arstingstall aided in assembling the experimental arrangement and acquiring data. Vish Katta from Innovative Scientific Solutions Inc. provided insightful conversations regarding inverse diffusion flames. Brian Bohan supplied the visible images of the flames.

8. References

[1] Zelina, J., Greenwood, R., Shouse, D., 51st ASME International gas Turbine and Aeroengine Congress and Exposition, paper 90119 (2006).
[2] Lukachko, S., Kirk, D., Waitz, I., *Journal of Engineering for Gas Turbines and Power* 125 (2003) 742-750.
[3] Kirk, D., Guenette, G., Lukachko, S., Waitz, I, *Journal of Engineering for Gas Turbines and Power* 125 (2003) 751-759.
[4] Anderson, W., Polanka, M., Zelina, J., Evans, D., Stouffer, S., Justinger, G., *Journal of Engineering for Gas Turbines and Power* 132 (2010) 051501.
[5] Lin, C.-X., Holder, R., Thornburg, H., Sekar, B., Zelina, J., Anderson, W., Polanka, M., Stouffer, S., Briones, A., *47th AIAA Aerospace Sciences Meeting*, Orlando, FL, 2009-678.
[6] Thornburg, H., Sekar, B., Zelina, J., Anderson, W., Polanka, M., Lin, C., Holder, R., Briones, A., Stouffer S., *47th AIAA Aerospace Sciences Meeting*, Orlando, FL, 2009-510.
[7] Partridge, W., Laurendeau, N., *Fuel* 74 (1995) 1424-1430.
[8] Clausing, E., Senser, D., Laurendeau, N., *Combustion and Flame* 110 (1997) 405-408.
[9] Wu, K.-T., Essenhigh, R., *Proceedings of the Combustion Institute,* 20 (1984) 1925-1932.
[10] Shaddix, C., Williams, T., Blevins, L., Schefer, R., *Proceedings of the Combustion Institute* 30 (2005) 1501-1508.
[11] Broadwell, J., Dahm, W., Mungal, G., *Proceedings of the Combustion Institute*, (1985) 303-310.
[12] Muppidi, S., Mahesh, K., *Journal of Fluid Mechanics* 598 (2008) 335-360.
[13] Bagheri, S., Schlatter, P., Schmid, P., Heningson, D., *Journal of Fluid Mechanics* 624 (2009) 33-44.
[14] Grout, R., Gruber, A., Yoo, C., Chen, J., *Proceedings of the Combustion Institute* 33 (2011) 1629-1637.
[15] New, T., Lim, T., Luo, S., *Experiments in Fluids* 40 (2006) 859-875.
[16] McMillin, B., Palmer, J., Hanson, R., *Applied Optics* 32 (1993) 7532-7545.
[17] Muppidi, S., Mahesh, K., *Journal of Fluid Mechanics* 530 (2005) 81-100.
[18] Chauduri, S., Kostka, S., Renfro, M., Cetegen, B., *Combustion and Flame* 157 (2010) 790-802.
[19] Cattolica, R. *Applied Optics*. 20 (1981) 1156-1166.
[20] Luque, J., Crosley, D.R., *SRI International Report* MP-99-009 (1999).
[21] Hanson, R.K., Seitzman, J.M., Paul, P.H., *Applied Physics B* 50 (1990) 441-454.
[22] Seitzman, J.M., Kychakoff, G., Hanson, R.K., *Optics Letters*. 10 (1985) 439-441.

[23] Evans, D., *Master's Thesis*, Air Force Institute of Technology, Dayton, OH 2008.
[24] Stouffer, S., Pawlik, R., Justinger, G., Heyne, J., Zelina, J., Ballal, D., *43rd AIAA/ASME/SAE/ASEE Joint Propulsion Conference*, Cincinnati, OH, 2007-5663.
[25] Bogard, D., Thole, K., *Journal of Propulsion and Power* 22 (2006) 249-270.
[26] CEA2, Chemical Equilibrium with Applications, Chemical Equilibrium Solver, NASA, Cleveland, OH (2004).
[27] Kostka, S., Roy, S., Lakusta, P.J., Meyer, T.R., Renfro, M.W., Gord, J.R., Branam, R., *Applied Optics* 48 (2009) 6332-6343.
[28] Westbrook, C., Proceedings of the Combustion Institute, 28 (2000) 1563-1577.
[29] Law, C.K., *Combustion Physics*, Cambridge Press, New York (2006) 94.
[30] Turns, S., *An Introduction to* Combustion, McGraw-Hill, Yew York (2000) 152.
[31] Katta, V., Stouffer, S., Roquemore, W., *Combustion and Flame*, 2010 (in press).
[32] Ben-Yakar, A., Hanson, R., *Proceedings of the Combustion Institute*, 27 (1998) 2173-2180.
[33] Huang, R., Yang, M., *Combustion and Flame* 105 (1996) 211-224.